Utilization of Medical Image Soft Segmentation Based on Fuzzy Sets Classification Process Modified by Local Aggregation Approach

J. Kubicek, M. Penhaker, M. Augustynek, I. Bryjova, J. Valosek
VSB–Technical University of Ostrava, FEECS, K450,
17. listopadu 15, 708 33, Ostrava–Poruba, Czech Republic.
jan.kubicek@vsb.cz

***Abstract*—Medical image segmentation has been a challenging task for a long time. In the current age, we are overcrowded by medical image data acquired from various sources, such as CT, MR, ultrasound and many others. We usually need to perform segmentation, detection and extraction of objects of interest for further processing. This process includes quantification of parameters to determine a clinical evaluation. There are multiregional segmentation methods that allow for differentiation of individual morphological objects. However, the commonly used hard thresholding approaches lack of robustness in noisy environment leading to an incorrect pixel classification. Image segmentation based on fuzzy set theory brings much more effective alternative for image thresholding gained by local aggregation, making this method more noise resistive. We consciously performed a comparative analysis of articular cartilage and blood vessels segmentation. It was an obvious method utilization in which the native image features are badly recognizable and the objects features are well observed.**

***Index Terms*—Fuzzy Sets; Fuzzy Thresholding; Image Segmentation; Local Aggregation; Articular Cartilage; Blood Vessels; Calcification; Arthritis.**

I. INTRODUCTION

In the field of medical image processing, the image segmentation is an important task as it leads to the extraction of object of interest. For this task, the multiregional segmentation based on the thresholding is frequently used. This approach divides an input image into several disjoint regions with the aim of features extraction. Medical image data are often accompanied with noise and artefacts, which deteriorate an image quality and segmentation results as well. These facts lead to the incorrect segmentation, which is linked with less accuracy of extracted image features. [20]

The main limitation of a global image thresholding is the fact that pixels having the same level of brightness are always segmented into the same class. This fact can lead to an incorrect classification, especially in the cases where a noise is presented. This problem may be overcome by taking into account spatial information that describes the behavior of each pixel. [16]

The utilization of global information is demonstrated in Figure 1, where the pixel was classified as belonging to the class 3 indicated by red. In the pixel neighbourhood, it can be proved that pixel represents an isolated value probably generated by the noise image. A correction of this improper classification can be carried out by using the image information (noise model, probability of classification, distance to centroid), or utilizing the spatial or morphological information. In the case of applying the median filtration, pixel will be classified as class 1 indicated by blue. Similar result can be achieved by using the morphological dilatation. In these cases, important image information is missing. As shown in Figure 1, it is obvious that the red pixel probably belongs to class 1, and at the same time it is less probably that the pixel belongs to class 2. Segmentation method based on fuzzy sets theory is optimized, so that it takes into account the pixel local properties for classification method optimization. [14, 15]

Segmentation method based on the fuzzy set theory, also called as the soft classification approach, generates the classification multiregional model base on the individual recognizable image areas separation. The core of the method is based on the fact that each class (for each region) is formed on the base of the fuzzy trapezoidal function assigned to each pixel of a certain membership value. As a result, we obtain transformation of the pixel spatial information to a membership plane. It is different from the hard thresholding approaches that involve assigning pixels to respective classes. This procedure is followed up by the local aggregation, where each membership function is modified on the base of local information. Theoretically, the aggregation step could have been omitted. Nevertheless, this final step of segmentation procedure ensures classification robustness, especially, for the cases where noise is presented, and it is supposed that the noise pixels would have been classified into improper class. [1, 2, 3, 4, 5]

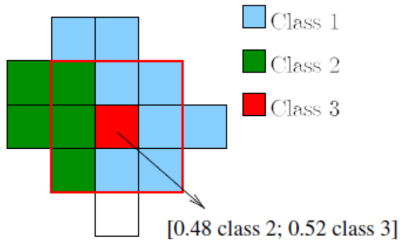

Figure 1: Example of noise pixel classification on the base of the hard thresholding approach [7]

II. SOFT SEGMENTATION BASED ON FUZZY SETS THEORY

It is supposed that image is described by the mathematical model $I(x, y)$, where x and y correspond with the horizontal, respective vertical pixel coordinates. In the following description, it is used *I(r)* for discrete image matrix composed of *L* incompatible regions which should be extracted so that we achieve the segmented model:

$$M(r) = g_s\{I(r)\} \tag{1}$$

where $g_s\{.\}$ depicts the segmentation method, which can be perceived as the function mapping of N_I monochromatic image levels into *L* regions i.e. $N_I \rightarrow L$, where $L < N_I$. After performing the segmentation, it is supposed that each pixel of an input image has certain membership level in L^{th} region. In the following description, we use $\mu_l(x), l=1,\ldots,L$ for a fuzzy function of l^{th} region. The overall segmentation method (Figure 3) comprises of the five essential steps. [7, 8, 12]

A. Centroids Extraction

Individual regions generated by the process of segmentation are defined based on the use of *L* centroids. As mentioned before, the number of centroids is $L<N_I$. Every class is defined by a respective centroid. For this reason, in the initialization step, we need to define all centroids. For practical purposes of the centroid extraction, the K means method is used (Figure 2). The algorithm iteratively seeks vector values by the way that minimizes root mean square between the given dataset (pixels), and vectors (distance from point to cluster centroid) having the smallest Euclidean distance to this data. [6, 12]

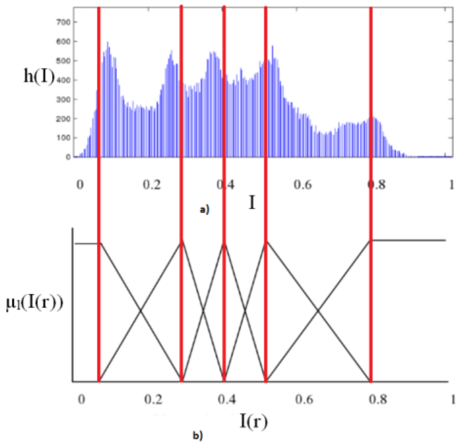

Figure 2: Process of histogram segmentation into predefined classes. (a) Example of normalized histogram, (b) approximation of histogram by sequence of triangular fuzzy membership functions $\mu_l(I(r))$ defined by extracted centroids on the base of K means method (red)

B. Membership Function

Fuzzy membership function is assigned to each of the classes, which are linked with the defined centroids. Theoretically, segmentation method could have used membership function based on an image histogram. The idea would be the approximation of individual histogram segments by the sequence of Gaussian membership functions. The main disadvantage of this approach is the working out of the mathematical optimization of particular parameters of distribution to achieve the minimal differences between the original histogram and the resulting approximation. Furthermore, it is excluded from using the unified distribution for variable image data because data from a particular image source have different image properties, and the structure of histogram is not identical. A better idea is using the pseudo trapezoidal function (PTS). This function is directly generated based on centroids. It represents a proper solution for the main purpose of segmentation or for the cases where we do not have information describing the intensity value of the distribution of particular tissues in the image.

C. Function Assigning to each pixel

Membership of pixel *r* in image *I(r)* is defined by the expression: $\mu_l(I(r))$. By using the PTS function, we have: $\sum_{l=1}^{L} \mu_l(I(r)) = 1$. At this point, the initialization phase of the thresholding can be done by the following expression:

$$M(r) = argmax_l\{\mu_l(I(r))\} \tag{2}$$

where *M(r)* represents the output of the segmentation model. In this way, the spatial information is not taken into account, and the result is strongly depended on a selected method of centroid extraction. The output of each pixel in this phase is given by a vector of membership functions:

$$\mu(I(r)) = [\mu_1(I(r))\ \mu_2(I(r)) \ldots\ \mu_L(I(r))]$$

In the case of using the PTS functions, only two elements of each vector are nonzero.

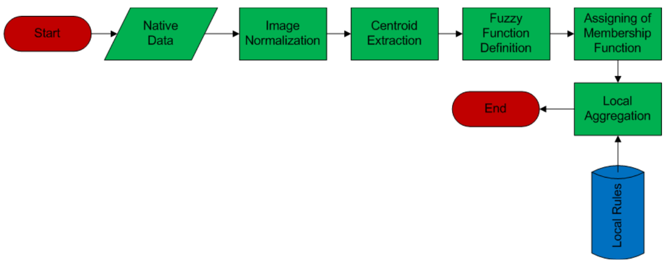

Figure 3: Flow chart of soft segmentation method for image thresholding [9, 10, 12]

D. Local Aggregation

Before generating the final segmentation step, it is necessary to take into account the spatial information. This step consists of the main contribution in the whole method. A versatility of the fuzzy logic allows for the design of many different ways of considering the pixel neighborhood from the membership levels $\mu(I(r))$ defined in the previous description. We suppose that $\eta(r)$ is a pixel neighborhood centered in the surrounding of pixel *r*. A local aggregation is defined by the following expression:

$$\mu^S(I(r)) = agg_{s\in\eta(r)}\{\mu(I(s))\} \tag{3}$$

where $agg\{.\}$ represents fuzzy aggregation in the pixel neighborhood $\eta(r)$. The main purpose of this function is the modification of original membership function $\mu_l(I(r))$ where local information is taken into account. The important feature of this operation is the fact that it works in the area of fuzzy membership functions. [18, 19]

E. Problem of Noise Pixel Classification

The soft thresholding algorithm might have been terminated in the step of assigning the membership level to each pixel, which consequently, the pixel would have been classified into respective class based on a maximal value of a membership function. This classification would have weakly reflected the influence of the noise pixel. From the view of the noisy pixels manifestation, it is supposed that their brightness spectrum is significantly different from the spectrum of a certain object, which should be segmented. For this reason, noisy pixels substantially deteriorate native image data. Since the noise spectrum is significantly different from the observed image objects, we can suppose that noise pixels will also have significant different level of membership function for a particular area against the other pixels in the object.

0.9	0.8	0.9
0.7	1	0.9
0.7	1	0.9

(a)

0.9	0.8	0.9
0.7	0	0.9
0.7	1	0.9

(b)

Figure 4: Neighborhood (3x3) of analyzed pixel indicated by red, (a) it is not supposed noise (b) analyzed centered pixel representing of noise element

It is obvious that in situations where we do not expect the presence of noise, the other pixels have higher membership values for that particular region (Figure 4(a)). In the case where the noise pixel is present, we can suppose that this pixel has zero level of membership value for the analyzed region because it has significantly different level of brightness function. Apparently, it would have been classified into different region. This phenomenon would have appeared itself as artifact (Figure 4(b)). This unfavorable fact is compensated by the use of local aggregation that reflects the spatial information of membership function. The main task of the local aggregation is the modification of originally assigned membership value based on the information of adjacent pixels. Since the membership function of noisy pixel is significantly different against the analyzed region pixels, an operator that is robust against outlying observation should be used. A suitable alternative for this situation is the use of median. The current value of the centered pixel is calculated based on the median from the surrounding pixels (Figure 5).

0.9	0.8	0.9
0.7	0.9	0.9
0.7	1	0.9

(a)

0.9	0.8	0.9
0.7	0.9	0.9
0.7	1	0.9

(b)

Figure 5: Value of membership function on the base of median of analyzed pixel indicated by red, (a) it is not supposed of noise level presence, (b) analyzed centered pixel representing of noise element

Based on the median operation, it is evident that the membership value is less variable than its surrounding. It is fractionally modified, and we can suppose that this change will not influence the resulting segmentation effect (Figure 5(a)). In the case of noise pixel membership function modification, a significant change is achieved. An original noise pixel had zero level of membership function for a given region, after applying the median operation membership level that converges to the centroid of analyzed region (Figure 5(b)).

F. Median Aggregation

A membership of each pixel in *η(r)* is "aggregated" based on the median aggregation. The formulation uses the following expression:

$$\mu_l^s(I(r)) = median_{s\in\eta(r)}\{\mu(I(s))\} \quad (4)$$

We should note that the neighborhood *η(r)* could be oriented so that it would be possible to find the structures in one particular direction.

G. Image Segmentation

The final step of the method deals with the calculation of the final segmented image based on the modified membership functions. In this final step, it used the maximum operator, given by the following expression [7, 13]:

$$M(r) = \arg max_l\{\mu_l^s(I(r))\} \quad (5)$$

III. MEDICAL IMAGE SEGMENTATION

We are devoted to the analysis, segmentation and extraction of articular cartilage and blood vessel system. We consciously state these two issues deal with different task in the context of data structure.

The first issue deals with the analysis of articular cartilage. Articular cartilage is clinically imagined by MRI due to higher contrast in comparison with other methods (X-ray, ultrasound). The major task is the differentiation of cartilage structure and localization of cartilage deteriorations. Cartilage is investigated, especially, due to suspicion of arthritis presence. This disease is clinically classified into four stages based on seriousness. From the view of image processing, it is the most interesting early deterioration of cartilage (I. stage). In this stage, arthritis is badly observable from the native records by a naked eye even for the clinical experts. Furthermore, in the clinical practice, the absence of SW instruments allows for processing native records from MR. The output of this analysis is a mathematical model reflecting individual tissues with the target of localization, followed up by the extraction of pathological interruptions at the early stage. A mathematical model shall reflect the individual areas of articular cartilage classified into individual classes in the area of artificial color map.

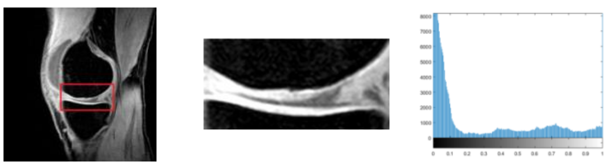

(a) (b) (c)

Figure 6: Native MR cartilage data acquired from PD (proton-dense) sequence with RoI indicated by red (a), RoI with adaptive interpolation (b), normalized histogram of selected area of interest (c)

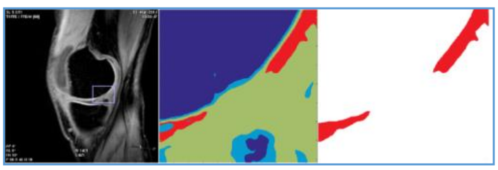

Figure 7: Native MR cartilage data where part of the cartilage with early deterioration is indicated by square (left), result of soft segmentation model, where four classes are used (middle) and final model of articular cartilage (right)

Figure 7 shows the loss (delamination) of dorsal part articular cartilage. Cartilage deterioration is badly recognizable from the native data. Model of articular cartilage precisely differentiate the individual structures of knee area. In the context of our analysis, the most important structure is indicated by the red color representing the part of articular cartilage. It is obvious that the mathematical model allows a precise differentiation of cartilage without damage (red color), and spot of missing cartilage (gaps).

The second issue deals with the blood vessels extraction, and differentiation of pathological structures. We process the blood vessel images acquired from CT angiography. Blood vessels are corrupted by calcification changes. Calcification is manifested since the white structure is significantly visible in comparison with the physiological part of blood vessels. The important task for the clinical practice is the automatic detection blood vessel area and the differentiation of physiological part from the calcified area. Sample of the testing images from our database is depicted in Figure 8.

Figure 8: Native CT angiography blood vessel images. Blood vessels are corrupted by calcification changes indicated by white color.

In the context of blood vessel calcification, there is a clinically important parameter that describes the level of calcification. This parameter is called calcium ratio. In clinical practice, the level of calcification is only estimated by a naked eye without any software feedback. Our analysis serves as an initialization phase for the quantification of areas that corresponds with the pathological changes.

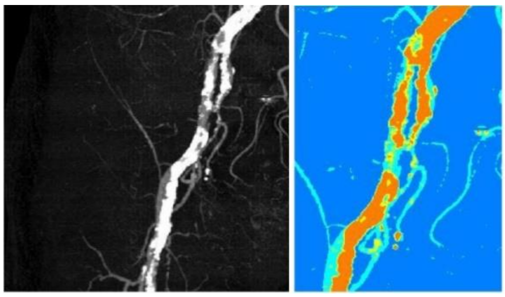

Figure 9: Native CT angiography blood vessel image (left) and mathematical model based on the soft segmentation (4 classes), calcification is indicated by beige color (right)

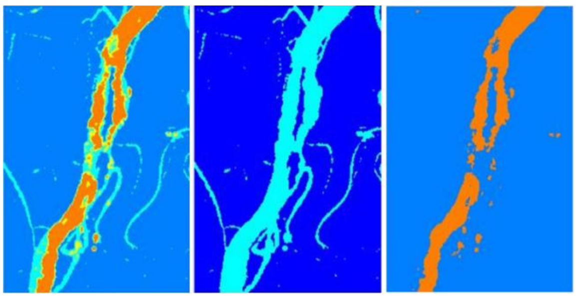

Figure 10: Model of whole blood vessel (left), model of physiological part of the vessel (middle) and calcification model (right)

IV. Quantitative Comparison

A quantitative comparison of the soft segmentation method was performed against a well-known thresholding method, including Otsu hard thresholding for *N* regions (Otsu-N), Fuzzy C-means (FCM) and Iterative thresholding segmentation (ITS) on the sample of blood vessels (CT) and cartilage data (MR). For a quantitative comparison, the following scalar measures were used:

- Rand Index (RI): it measures similarities between two data clusters. *RI* compares a compatibility of assignments between pairs of elements in two clusters. [21]
- Variation of information (VI): it determines a distance between two segmentations in the sense of their average conditional entropy. [21]

Table 1
Quantitative comparison of multilevel segmentation methods

	Otsu-N	FCM	ITS	MedAg
RI	0.771	0.779	0.561	0.781
VI	2.899	2.998	2.656	2.642

Table 1 shows a quantitative comparison of the soft segmentation methods with a median aggregation (MedAg) against the standard multilevel methods that represents a gold standard in this area. Note that for higher result of *RI* measure indicates better performance. Contrarily, in the case of *VI*, a small figure indicates a better result. Based on the quantitative comparison, we can state that the soft thresholding method seems to be promising in the application of medical image data.

V. Conclusion

We analyzed segmentation approach, which is reliable and useful in the area of medical image processing. There are many methods, which lead to the hard thresholding approach where each pixel is classified based on a hard decision. The presence of noise is a significant problem in the context of proper segmentation because it is nearly impossible to perform correct classification pixels that have different intensity properties than the pixels that belong to the analyzed object. The soft segmentation approach utilizes the feedback by incorporating the spatial information of every segmented pixel. This approach appears itself as effective, especially, during the presence of noise. It is well known that each medical image generated by certain medical imagining alternative is accompanied by noise related to respective physical method; therefore, segmentation method that takes into account the noise information is very effective. Soft segmentation method is sufficiently effective: It is proven on articular cartilage, where the pathological changes are badly recognizable, despite its segmentation model is able to precisely separate the pathological changes at the early stage. The second important issue is the extraction of calcification changes since it would be possible to objectively quantify calcium score as an indicator of blood vessel deterioration.

Acknowledgment

The work and the contributions were supported by the project SV4506631/2101 'Biomedicínské inženýrské systémy XII'.

REFERENCES

[1] R. Thota, S. Vaswani, A. Kale, N. Vydyanathan, Fast 3d salient region detection in medical images using GPUS (2016) *Advances in Intelligent Systems and Computing*, 390, pp. 11-26.

[2] S.Zhang, D. Metaxas, Large-Scale medical image analytics: Recent methodologies, applications and Future directions (2016) *Medical Image Analysis*, 33, pp. 98-101.

[3] D. Rueckert, B. Glocker, B. Kainz, Learning clinically useful information from images: Past, present and future (2016) Medical Image Analysis, 33, pp. 1339-1351.

[4] Q.Wen, S. Xu, S. Wan, Ultrasound image segmentation based on energy functional (2016) *Journal of Nanoscience and Nanotechnology*, 16 (9), pp. 9359-9370.

[5] Y. Deng, F. Bao, X. Deng, R. Wang, Y. Kong, Q. Dai, Deep and Structured Robust Information Theoretic Learning for Image Analysis (2016) *IEEE Transactions on Image Processing*, 25 (9), art. no. 7506023, pp. 4209-4221.

[6] S. C. Yang, Y.-J. Wun, Y.-J. He, Designated target enhancement and segmentation in multi-spectral MR images(2016) Proceedings - 2016 *IEEE International Symposium on Computer, Consumer and Control, IS3C 2016*, art. no. 7545377, pp. 1059-1062.

[7] J. Kubicek, M. Penhaker, I. Bryjova, M. Kodaj, Articular cartilage defect detection based on image segmentation with colour mapping (2014) Lecture *Notes in Computer Science (including subseries Lecture Notes in Artificial Intelligence and Lecture Notes in Bioinformatics)*, 8733, pp. 214-222.

[8] J. Kubicek,, M. Penhaker, I. Bryjova, M. Augustynek, Classification method for macular lesions using fuzzy thresholding method (2016) *IFMBE Proceedings*, 57, pp. 239-244.

[9] J. Kubicek, J. Valosek, M. Penhaker, I. Bryjova, Extraction of chondromalacia knee cartilage using multi slice thresholding method (2016) *Lecture Notes of the Institute for Computer Sciences, Social-Informatics and Telecommunications Engineering, LNICST*, 165, pp. 395-403.

[10] J .Kubicek, J.Valosek,, M. Penhaker, I. Bryjova, J. Grepl, Extraction of blood vessels using multilevel thresholding with color coding (2016) *Lecture Notes in Electrical Engineering*, 362, pp. 397-406.

[11] S. Aja-Fernandez, G. Vegas-Sanchez-Ferrero, M.A. Martin Fernandez,. Soft thresholding for medical image segmentation. (2010)

[12] M. Augustynek,, M. Penhaker, J. Semkovic, P. Penhakerova, M. Cerny, Measurement and Diagnosis Assessment of Plethysmographycal Record. In 5th Kuala Lumpur *International Conference on Biomedical Engineering (BIOMED 2011)*. Kuala Lumpur, MALAYSIA, 2011, vol. 35, p. 320-323.

[13] J. Kubicek, M. Penhaker, Fuzzy Algorithm for Segmentation of Images in Extraction of Objects from MRI, 2014 *International Conference on Advances in Computing, Communications and Informatics (Icacci)*, pp. 1422-1427, 2014.

[14] Z. Rezaei, A. Selamat, M. S. M. Rahim, and M. R. A. Kadir, Image Segmentation of Coronary Artery Plaque Using Intuitionistic Fuzzy C-Means Algorithm, *Proceedings of International Conference on Artificial Life and Robotics (Icarob 2014)*, pp. 26-31, 2014.

[15] J. Blahuta, T. Soukup, M. Jelinkova, P. Bartova, P. Cermak, R. Herzig, et al., A new program for highly reproducible automatic evaluation of the substantia nigra from transcranial sonographic images, *Biomedical Papers-Olomouc*, vol. 158, pp. 621-627, 2014.

[16] M. Cerny and M. Pokorny, Circadian Rhythm Evaluation Using Fuzzy Logic, in *Advanced Methods for Computational Collective Intelligence*. vol. 457, N. T. Nguyen, B. Trawinski, R. Katarzyniak, and G. S. Jo, Eds., ed, 2013, pp. 289-298.

[17] J. Nowakova and M. Pokorny, System Identification Using Genetic Algorithms, in *Proceedings of the Fifth International Conference on Innovations in Bio-Inspired Computing and Applications*. vol. 303, P. Kromer, A. Abraham, and V. Snasel, Eds., ed, 2014, pp. 413-418.

[18] P. Sispera, M. Pokorny, and J. Roupec, T-S fuzzy modelling using advanced genetic algorithms, 2005.

[19] H. Sun, Y. Ma, H. Wu, L. Miao, X. Chen, X. Ji, P. Cai, P. An improved OTSU's method for CT image boundary contour extraction (2016) IST 2016 - 2016 *IEEE International Conference on Imaging Systems and Techniques*, Proceedings, art. no. 7738276, pp. 493-497.

[20] M. Meila, Comparing clustering: an axiomatic view, in: *Proc. of the 22nd International Conference on Machine Learning*, New York, NY, USA, 2005, pp. 577–584.

[21] P. Arbeláez, M. Maire, C. Fowlkes, J. Malik, Contour detection and hierarchical image segmentation, *IEEE Trans. Pattern Anal. Mach. Intell.* 33 (5) (2011) 898– 916.